# Controlled Surface Assembly of Tobacco Mosaic Virus via Evaporation

SENIOR HONORS THESIS

Porakrit Leophairatana

TUFTS UNIVERSITY
Department of Chemical Engineering

April 25th, 2013

## Abstract

In this thesis, I examined two routes in controlling the surface assembly of genetically modified tobacco mosaic virus (TMV) towards the creation of uniform and well-ordered 2-D arrays with high density and alignment. As a highly robust and well defined rod, TMV is an excellent candidate as a building block for surface assembly and fabrication of functional nanobio-devices. Dynamic self-assembly, via controlled solvent evaporation, was exploited as a facile route to assemble TMV onto the glass surfaces. In the first route, varying the concentrations of TMV and sodium phosphate led to control over TMV density, alignment, and percent coverage. In the second route, the temperature of the system was varied, leading to direct control over TMV array density and alignment. Atomic force microscopy (AFM) and contact angle measurements were employed for surface characterization. Via this fabrication method, I created well-ordered TMV arrays with very high density and nearly 100% surface coverage. I envision that my scheme to create well-controlled TMV array will open doors for the development of functional devices based on nanobio-materials.

# Table of Contents

## Acknowledgements

Firstly, I would like to express my sincerest and deepest gratitude to Professor Hyunmin Yi for guiding me through my entire thesis, with his unending invaluable advice, wisdom, and patience. He was able to discern the weaknesses in my skills and, accepting them, exhorted me to dedicate more efforts into overcoming them. His belief and encouragements were my driving force to pursue and finish my senior honors thesis. Moreover, I would like to thank Professor Matthew Panzer for his excellent counsel that helped move my project forward. I would also like to thank my lab group members, Cuixian Yang, Sukwon Jung, JaeHun Lee, and John Abel for their assistance, support, and motivation. I want to thank Stephany Tsao for always motivating and supporting me. Lastly, I owe my parents and sisters so much for their constant support and caring, strong motivation and belief in my abilities.

# 1. Introduction

### 1.1 Motivation and Goal

The self-organization of biological macromolecules into well-ordered configurations has attracted a great level of interest in the past few decades due to its wide potential applications from electronic conduction[1], to catalysis[2], to sensing and diagnosis[3]. In particular, tobacco mosaic virus (TMV) is an excellent building block for assembly because of its well-defined structure and precisely controlled functionalities[4]. After years of intense research, it has been reported that TMV is able to self-assemble on several inorganic surfaces such as surface modified mica, silica, or gold[5,6]. Furthermore, the self-assembly of TMV in the oil or water interface has also been examined[7]. Specifically, with controlled evaporation, one can self-assemble TMVs onto glass capillary tubes or flat surfaces to create hierarchically ordered two dimensional (2D) arrays[8,9].

Despite the enormous progress, however, the ability to control the assembly of TMV is currently still lacking. There is little or no control over the density, distribution, or alignment of TMV onto surfaces. Also, difficulties arise when attempting to increase density and coverage of TMV because the viruses often form multilayers. Another major challenge arises in the attempt to create TMV arrays in a long-range, uniform, and defect-free fashion onto a substrate. The ability to control the assembly of TMV is very desirable in developing novel biomaterials; however, the current lack of control and understanding of how to control TMV assembly has hindered further development and applications of TMV arrays.

In light of this challenge, the purpose of my thesis is to use the fundamental principles of thermodynamics and colloidal chemistry to develop a simple scheme to control the assembly of genetically modified TMV towards the creation of uniform and well-ordered 2-D arrays with high density and alignment. Dynamic self-assembly, via controlled solvent evaporation, was exploited as a facile route to assemble TMV onto the glass surfaces. In this report, I examined two simple routes to control the surface assembly of TMV as shown in the schematic diagram of figure 1.1 on the next page. In the first route, varying the concentrations of TMV and sodium phosphate led to tunable surface assembly of TMV. By simply varying the concentrations of both, I was able to control the density, alignment, and distribution of TMV onto surfaces. Via this fabrication method, I created TMV arrays with very high TMV density and coverage (nearly 90%), exceeding those of other existing TMV surface self-assembly methods[2,5,6,8,10]. In the second route, the temperature of the system was varied, leading to direct control over TMV array density and alignment. AFM results show that at high temperature, the viruses aligned uniformly at high density and coverage (nearly 100% coverage), while at low temperature, they assembled randomly at low density. Finally, I show that slow evaporation speed was required to create well-ordered TMV arrays. I envision that my schemes to control the assembly of TMV will open doors for the development of functional devices based on novel nanobio-materials.

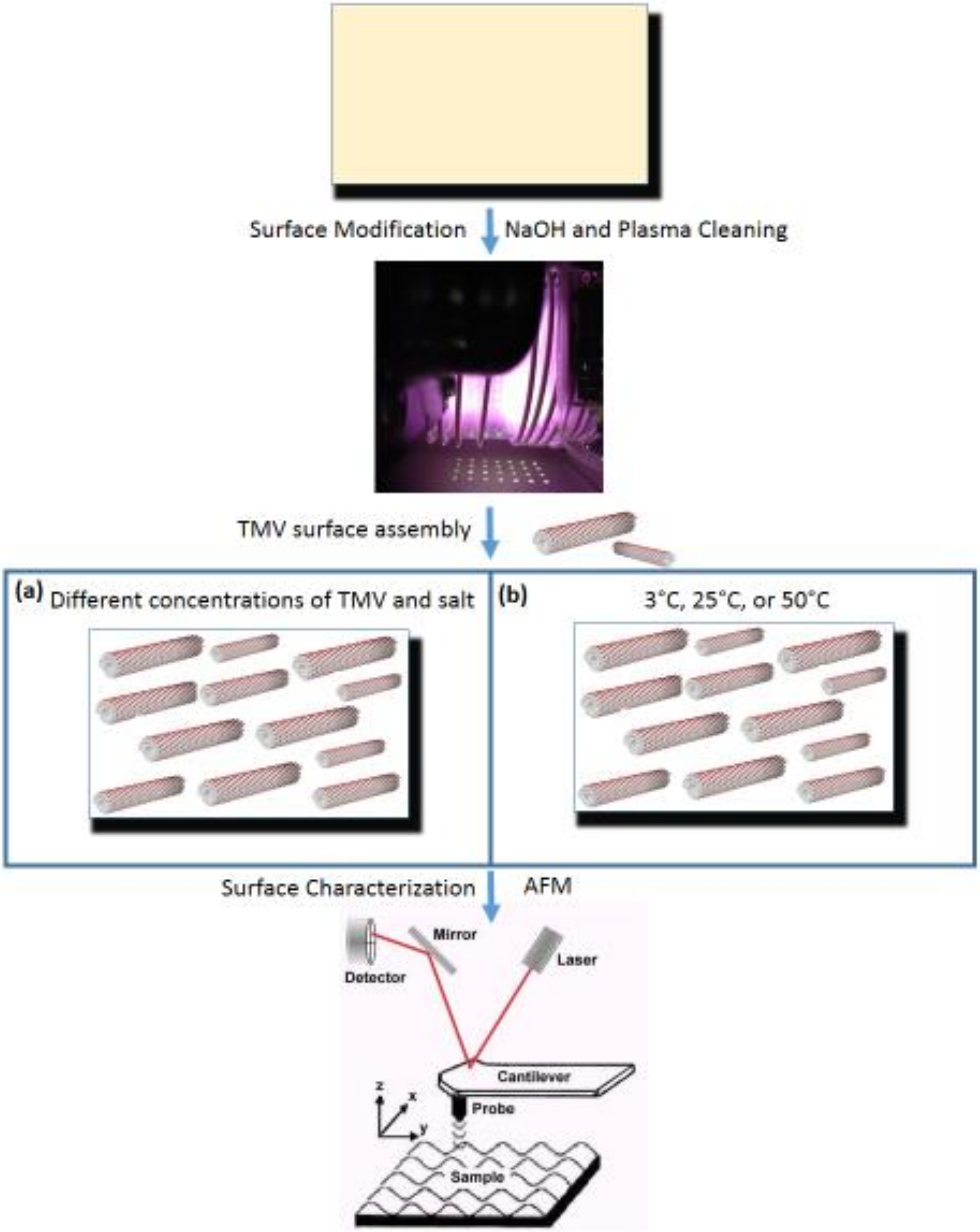


**Figure 1.1:** Schematic diagram of the process to create and characterize 2-D TMV arrays. Two methods were proposed for controlling the assembly of TMV: (a) varying the concentrations of TMV and sodium phosphate for surface assembly, and (b) regulating the temperature of the system during TMV assembly

## 1.2 Background

### 1.2.1 Tobacco Mosaic Virus

Tobacco Mosaic Virus (TMV) is a positive-sense single stranded RNA virus that is 300nm in length and 18 nm in diameter. It is composed of 2130 identical coat proteins, containing amine, hydroxyl, and carboxylate groups, encapsulating the RNA[11]. TMV is remarkably stable in wide ranges of temperature, acidity, and organic solvents, and used extensively as templates for the binding and deposition of a wide variety of inorganic and organic materials[1,2,4,11,12]. Particularly, TMV can be genetically modified to incorporate cysteine residues near the amino-terminus of the virus coat protein, which provide precisely spaced thiol functionalities enhancing the metal binding and nucleating capabilities of the TMV for assembly and deposition of metal nanoparticles[12]. The unique chemical properties, the well-defined structure, and the precisely controlled functionalities of the TMV make it an excellent candidate as a building block for surface assembly and fabrication of functional nanobio-devices.

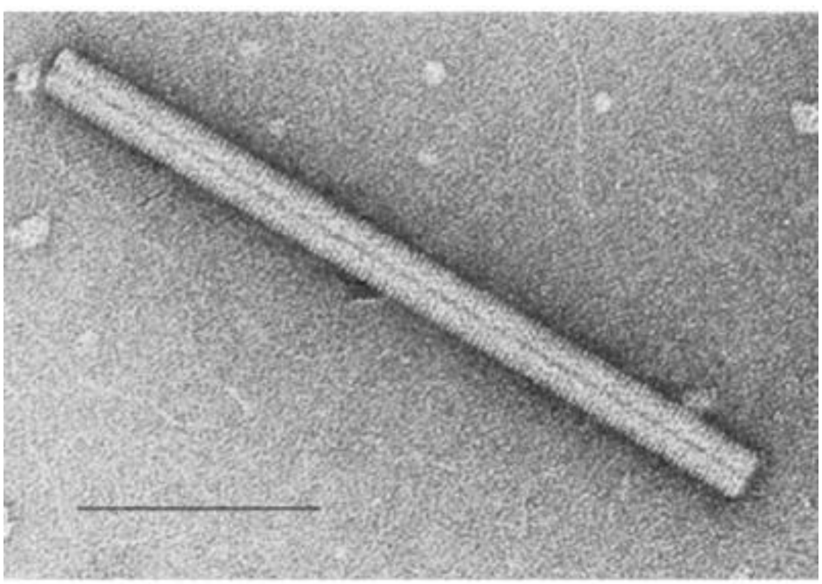

**Figure 1.2:** Electron Micrograph of Tobacco Mosaic Virus[13]

### 1.2.2 TMV Assembly

Dynamic self-assembly, via controlled solvent evaporation, was exploited as the facile route to assemble TMV onto the glass surfaces[9]. This alignment process utilizes the Coffee ring effect which is produced due to the pinning of the contact line onto the substrate by the solute[14]. In order to compensate for the evaporation of solvent at the liquid surfaces, liquid from the center is drawn to the edge at the three phase contact line. The capillary forces that pull the liquid to the surface also brings along TMV, which do not evaporate with the solvent. Thus, TMV density is increased locally at the liquid surfaces. With higher TMV density, free energy is found to be unstable if it is in isotropic distribution[15]. Higher TMV concentration has rotational and translational constraints in a way that "the freedom to rotate restricts the freedom to translate."[15] Therefore, the total entropy is maximized when the TMV sacrifices its rotational freedom to achieve higher translational freedom. Thus, with higher TMV concentration, the cylindrical rods are aligned in a nematic distribution parallel to the three phase contact line. Grzybowski and coworkers were able to show that nematic distribution occurs at the critical concentration when density of colloidal particles increases beyond $1/(\pi h^2 D)$, where h is the height of the TMV, and D is its diameter[15]. Utilizing the dimension of TMV ($18\times300 nm^2$) and the molecular weight of TMV of approximately 40MDa, the critical concentration of TMV was calculated to be 13 mg/mL (calculations shown in appendix 5.1). As the TMV solution evaporates, the viruses are deposited onto the hydrophilic glass surface via adsorption (non-specific binding) creating well-ordered TMV arrays.

# 2. Methods

## 2.1 Instrumentation

The original TMV1cys stock was generously provided by Professor James Culver's group from the University of Maryland's Institute of Bioscience and Biotechnology Research (IBBR). The viruses were grown and purified and used as building blocks for surface assembly. Sodium phosphate buffer (pH 7.0) was prepared and diluted for the preparation of TMV solution. Glass slides were purchased from Fisher Scientific (2.5 x 7.5 $cm^2$, 1.0 mm thick). Sodium hydroxide 10$\pm$0.05 N Concentrate (Fisher Scientific) and plasma cleaner/sterilizer (PDC – 32 G, Harrick Scientific) were used for substrate preparation. An enclosed chamber, an oven (VWR International), and a glove bag were utilized to create closed systems to control air temperature and humidity for surface assembly. Anhydrous calcium sulfate (Hammond Drierite) and ultrapure nitrogen gas were used in controlling air humidity.

Tapping mode Atomic Force Microscopy (AFM) was used as the primary tool for the analysis of the TMV surface assembly. The AFM (Veeco Dimension V 3100) consists of a cantilever with a sharp probe that oscillates at a resonant frequency above the surface of the specimen. As the cantilever comes to close contact with the surface, a laser beam is reflected off the back of the cantilever and collected by a position sensitive detector. The output of the signal is collected by a differential amplifier and is used to calculate for the height and roughness of the specimen.

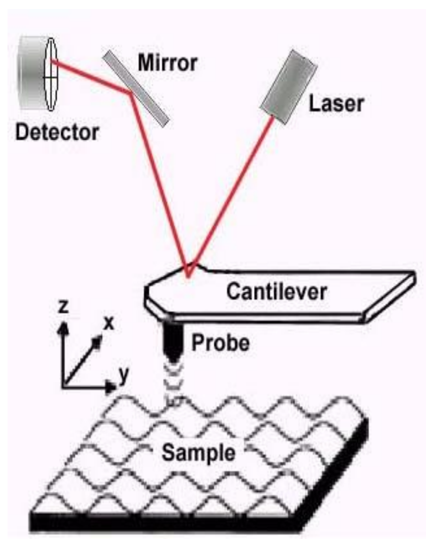


**Figure 2.1:** Tapping Mode Atomic Force Microscopy[16]

## 2.2 Substrate Modification

Glass slides were cut with a diamond glass cutter into 1.0 x 2.5 $cm^2$ spacers, 1mm in thickness. New glass slides often have organic and oil residues unevenly distributed on their surfaces, which make controlled and uniform evaporation of TMV solution difficult. In order to achieve clean, uniform, and hydrophilic glass surfaces, the glass slides and spacers were first cleaned in 10 N NaOH for 30 minutes, thoroughly washed with deionized water, and dried under ultrapure nitrogen gas. Treatment with sodium hydroxide makes the glass surface more hydrophilic since the hydroxide is able to remove hydrogen from the hydroxylated glass surface, exposing the polar oxygen group. After treatment with sodium hydroxide, the glass slides were then additionally cleaned with plasma cleaning at high power cleaning for 1.5 minute, in order to remove additional organic surface contaminations and create chemically active hydroxyl groups resulting in increased hydrophilicity. AFM and contact angle measurements were then used for surface characterization. After plasma cleaning, contact angle measurement showed uniform glass surfaces with contact angle of less than 1 degree throughout the entire surfaces, a significant drop from 20° prior to plasma cleaning. Figure 2.3 shows contact angle measurements with deionized water droplet on glass surfaces before and after plasma cleaning.

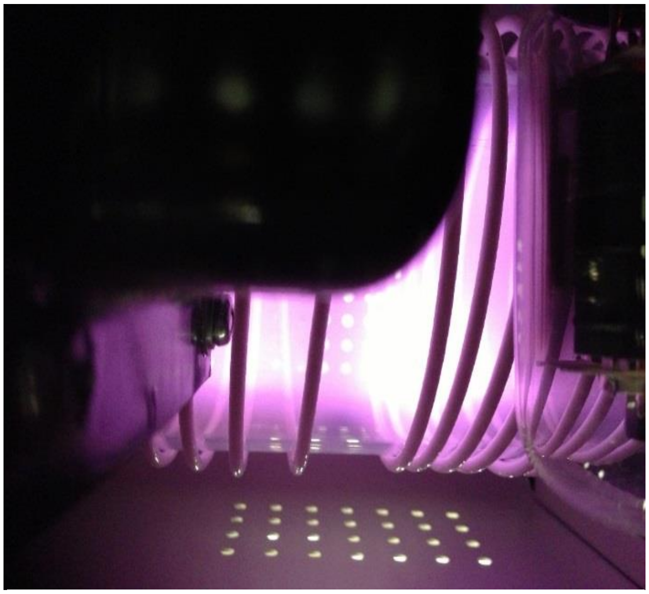

**Figure 2.2:** Image of plasma cleaner

(a)

(b)

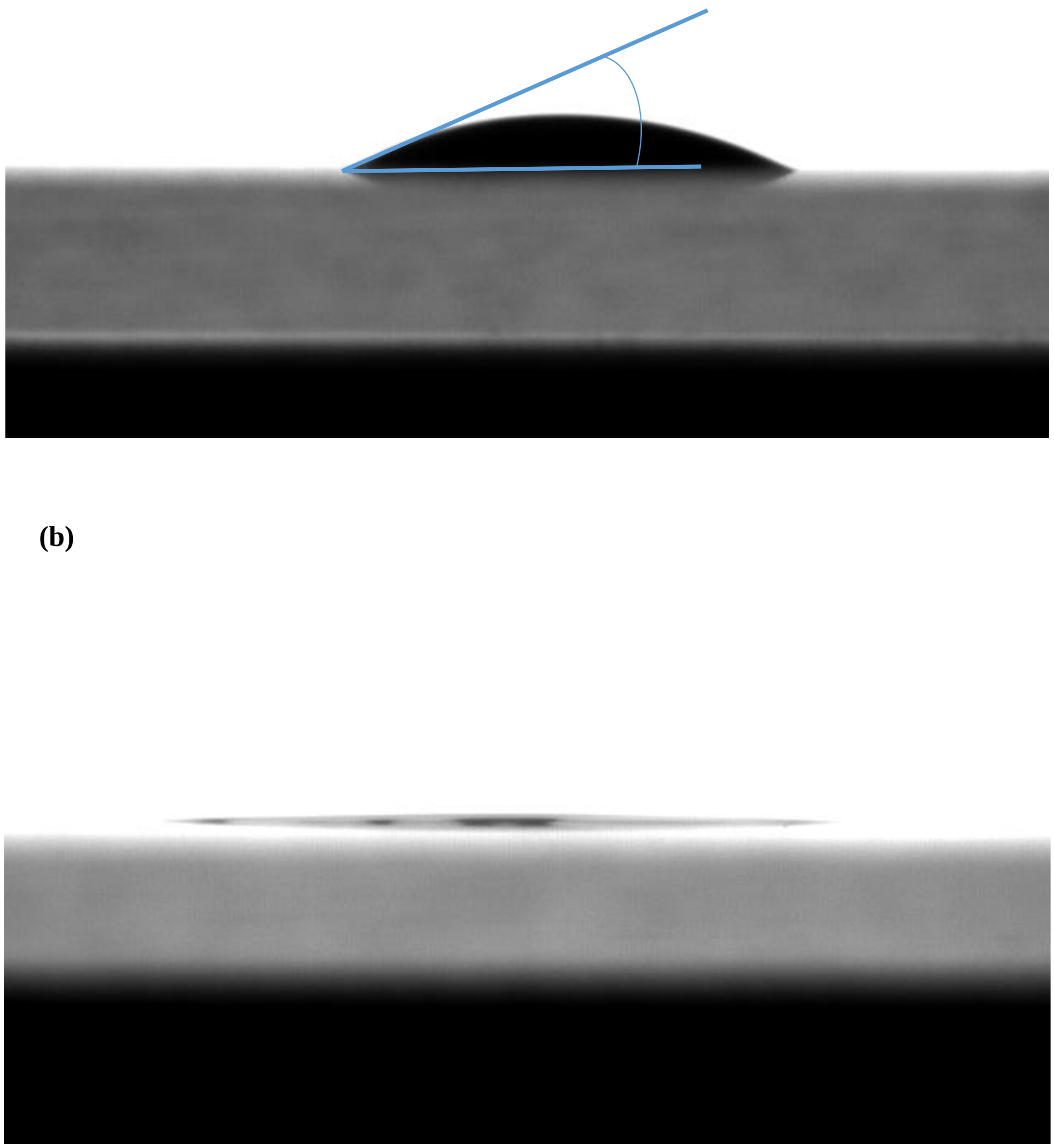

**Figure 2.3:** Image from contact angle goniometer. Water droplet on glass surfaces (a) before surface modification with plasma cleaning and (b) after surface treatment with plasma cleaning

## 2.3 TMV Assembly

### 2.3.1 TMV Assembly

Immediately after surface modification, two modified glass slides were horizontally stacked above one another with two spacers placed in between. 1.4 mL of TMV solution (normally 0.05mg/mL TMV in 0.01M sodium phosphate) was placed in a syringe and injected in between the two glass slides. The setup of the glass slides with spacers are shown by figure 2.4 below. In a typical experiment, the TMV assembly apparatus was then placed in a closed chamber at room temperature and constant humidity controlled at 50-60% relative humidity (RH). After approximately 2.5 days, the glass slides were then separated, thoroughly washed with DI water, and dried under ultrapure nitrogen gas for further surface characterization.

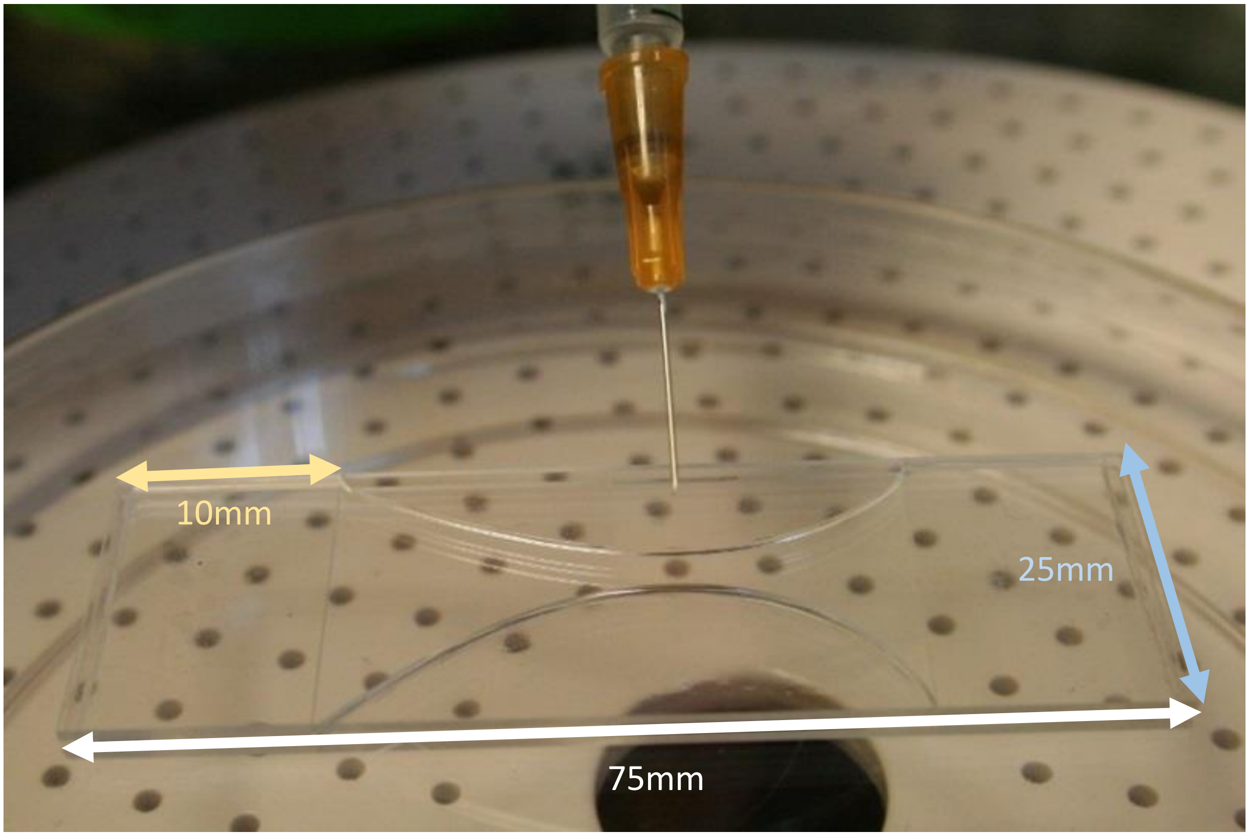


**Figure 2.4:** Image of TMV assembly setup

### 2.3.2 Temperature Variations

When low temperature (3ºC) was desired, the TMV solution was precooled to achieve thermal equilibrium. Then, it was injected in between two glass slide and allowed to dry in a closed chamber placed in a refrigerator with constant humidity controlled by adding anhydrous calcium sulfate (Hammond Drierite) into the chamber to keep humidity at 20-25% RH. At this temperature and humidity, total evaporation time took approximately 2.5 days. At high temperature (50ºC), TMV solution was first preheated. Then, it was injected in between two glass slides and allowed to dry in a closed chamber placed in an oven with temperature set at 50ºC. Humidity was maintained at 75-85% RH by adding extra water into the chamber. Approximately 2 days were required for the TMV solution to evaporate entirely. Then, the glass slides were separated, thoroughly washed with DI water, and dried under ultrapure nitrogen gas for further surface characterization.

### 2.3.3 Variation in Evaporation Rates

The effect of evaporation rates on TMV assembly were also examined at two different temperatures: 25ºC and 50ºC. In order to achieve rapid evaporation rate at higher temperature (50ºC), the TMV assembly apparatus was placed directly in an oven without a chamber lid. This resulted in low humidity (20% RH) and significant reduction in evaporation time of 3 hours. Then, to achieve high evaporation rate in room temperature, the TMV assembly apparatus was placed directly in a glove bag filled with ultrapure and prefiltered nitrogen gas. Humidity reduced significantly to 5-7% RH and evaporation time also dropped to 3 hours. After total evaporation, the glass slides were separated, thoroughly washed with DI water, and dried under ultrapure nitrogen gas for further surface characterization.

### 2.3.4 Modelling Evaporation Rates

In order to control the evaporation time, an empirical formula published by Willis Carrier and coworker was used to calculate the rate of evaporation (assuming the concentration of solute is negligible) as shown by equation (1) below[17,18]:

$$E = \frac{(0.0888 + 0.0783V)(Pw - Pa)}{hw} \qquad (1)$$

Where

E = Evaporation flux [kg/m$^2$sec]; Pw = saturated water vapor partial pressure [Pa]

Pa = water vapor partial pressure of air; hw = the latent heat of vaporization [J/kg]

For example, at room temperature, the saturated water vapor partial pressure is 2300 Pa. With humidity controlled at approximately 50% RH, water vapor partial pressure of air is calculated to be 1150 Pa. V=0 due to the absence of forced air flow and hw=2270000J/kg for the latent heat of evaporation. The evaporation flux was calculated to be E=162g/m$^2$hr. The rate of evaporation can then be calculated by multiplying the evaporation flux with the surface area of the liquid surface exposed to air. With initial evaporation rate calculated to be 0.018g/hr and maximum evaporation rate calculated to be 0.022g/hr, the process would require approximately 2.9 days in order to completely evaporate 1.4mL of water. Detailed calculations for the rate of evaporation can be found in appendix 5.2.

# 3. Results and Discussion

### 3.1 The Effect of Buffer Concentration and TMV Concentration on Assembly of TMV

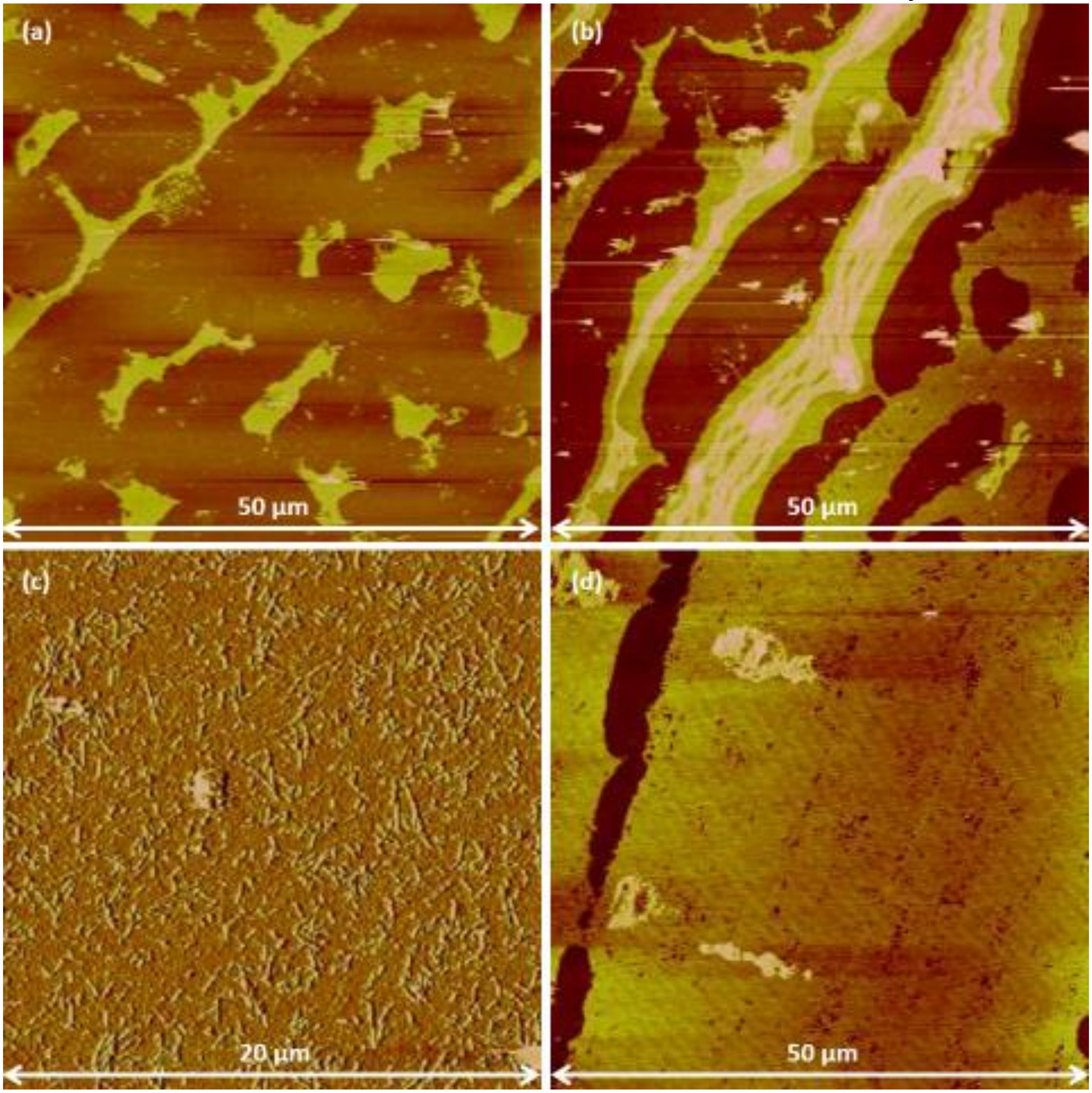


**Figure 3.1:** AFM images of TMV patterns formed during TMV assembly onto glass slides when TMV solutions were (a) 0.01mg/mL TMV in 0.1M sodium phosphate, (b) 0.05mg/mL TMV in 0.1M sodium phosphate, (c) 0.05mg/mL TMV in deionized water, and (d) 0.05mg/mL TMV in 0.01M sodium phosphate.

As shown in figure 3.1, I first examined a simple route to control TMV array percent coverage and alignment on glass surfaces by evaporating the TMV solution with varying concentrations of TMV and sodium phosphate for surface assembly. For this, solutions with different concentrations of TMV and salt were dried in between two glass slides to create enclosed space for controlled evaporation. Figure 3.1a shows that at low TMV concentration (0.01mg/mL) and high salt concentration (0.1M), the viruses were deposited in small stripe patterns with low density and coverage (areas on the AFM images that are yellow). Further high resolution AFM images and AFM height abundance confirm that these layers are indeed TMV arrays (figure 3.2a and figure 3.3). Quite interestingly, the height of the TMV was 33% less than its theoretical diameter of 18nm. Kern and coworkers, reported that the deformation of the adsorbed TMV on the glass surfaces serve to maximize the number of bonds of the TMV protein coat to the hydrophilic surfaces[20]. As shown in figure 3.1b, when TMV concentration was increased to 0.05mg/mL while maintaining the high salt concentration (0.1M), TMV coverage slightly increased. Higher resolution AFM images (Figure 3.2b), however, show that the viruses were assembled in multilayers, which was undesirable for surface assembly control. When salt concentration was reduced from 0.1M to 0.01M, TMV coverage increased significantly from approximately 50% (figure 3.1b) to 90% (figure 3.1d). Higher resolution AFM images confirmed that these layers are TMV array, and that they were aligned in monolayer with high density throughout the entire TMV stripes (figure 3.4). Figure 3.1c shows that with further reduction in salt concentration from 0.01M to 0M, the TMV assembled in isotropic distribution at low density. In short summary, figure 3.1 shows that decreasing the concentrations of sodium phosphate and TMV results in TMV array with lower density, lower alignment and less defined stripe patterns.

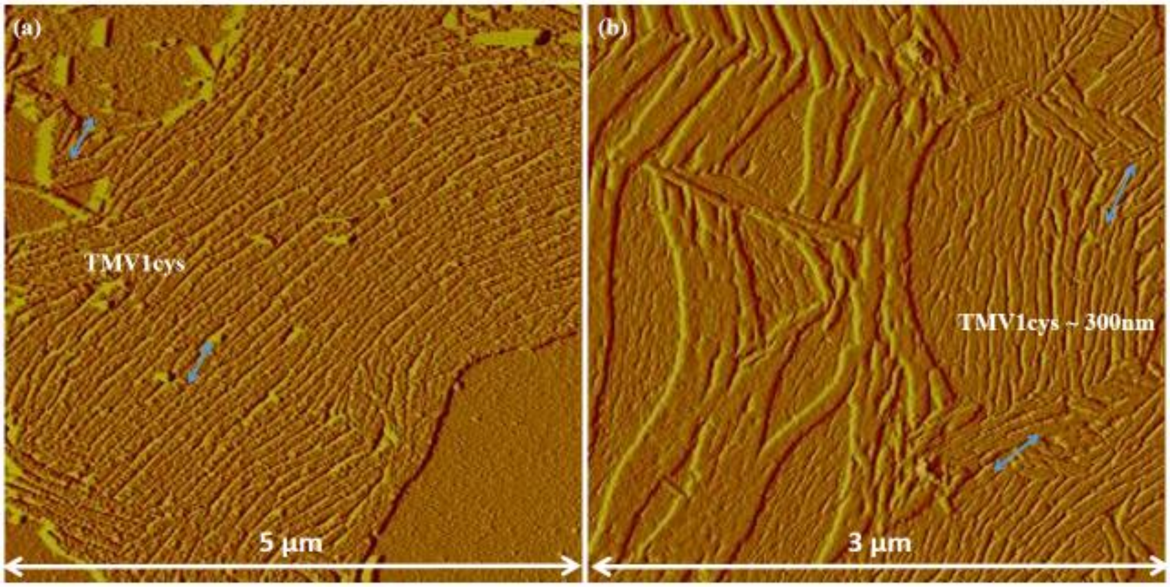


**Figure 3.2:** High resolution AFM images (amplitude error) of TMV patterns formed during TMV assembly onto glass slides when TMV solutions were (a) 0.01mg/mL TMV in 0.1M sodium phosphate, (b) 0.05mg/mL TMV in 0.1M sodium phosphate.  The length of the tubular rods were approximately 300nm, corresponding to that of TMV.

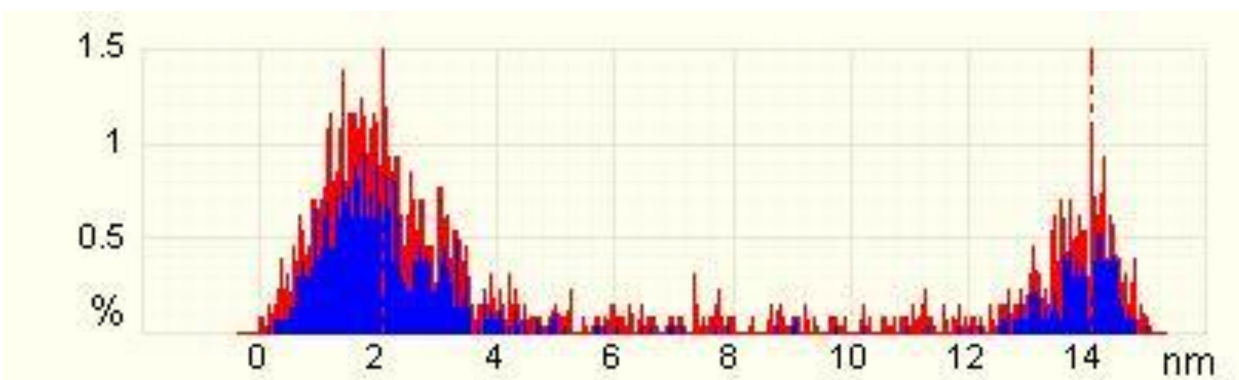


**Figure 3.3:** Relative abundance of surface heights from AFM image (figure 3.1a). The surfaces have two distinct heights: 2nm, corresponding to the relative height of glass surfaces and 14nm, corresponding to that of TMV array. Actual TMV array height is the difference of the two values, approximately 12nm.

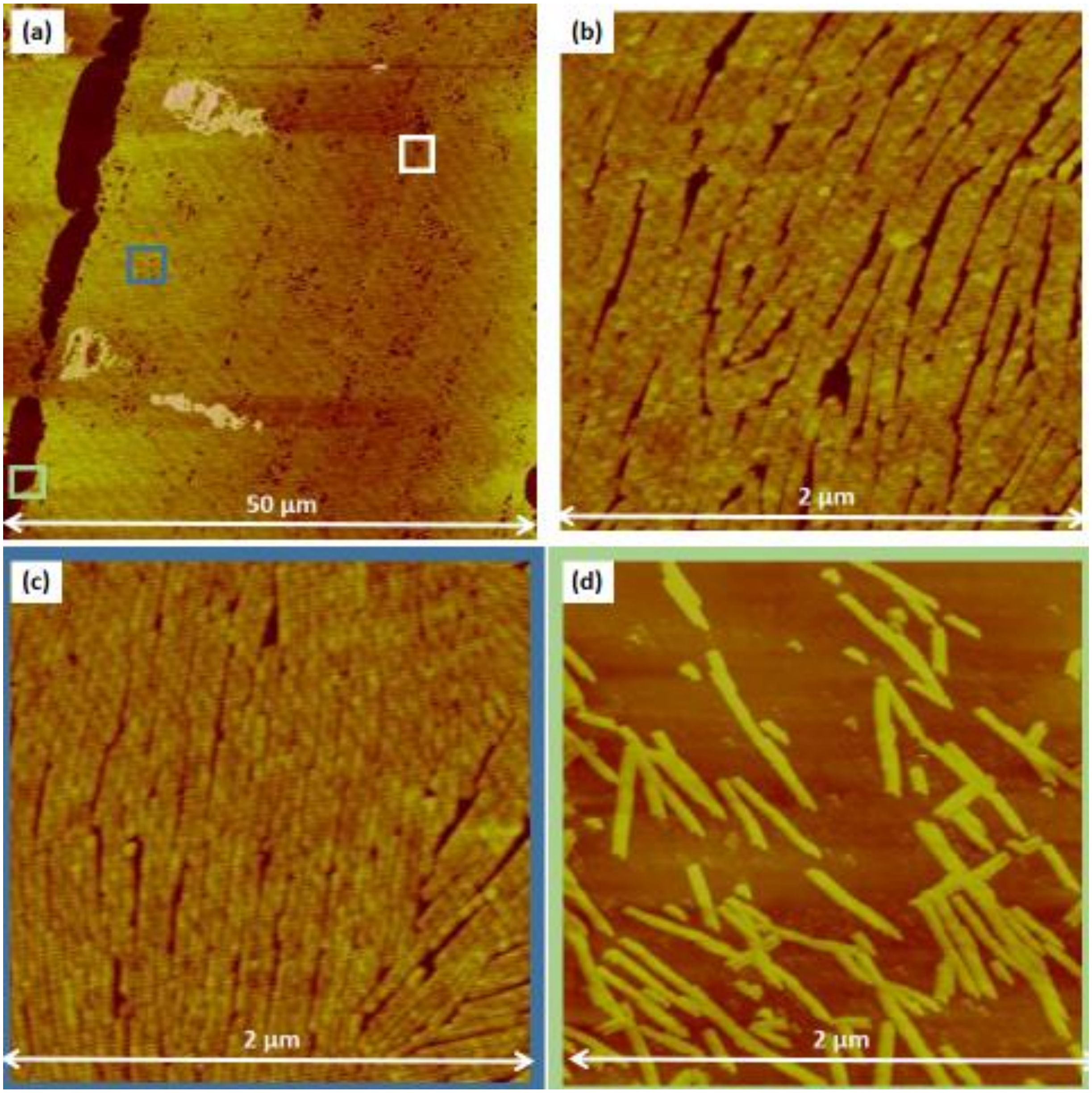


**Figure 3.4:** (a) AFM tapping mode image (height) of TMV array. (b) AFM image (height) of TMV array taken from the center of the TMV stripe. (c) AFM image (height) of TMV array taken near the side of the TMV stripe. (d) AFM image (height) taken from outside the TMV stripe

Firstly, figure 3.1 suggests that the presence of electrolyte was responsible for the formation of stripe patterns during the drying of TMV solution. For better clarification, TMV stripes are defined as bundled TMV arrays with one directional orientation, ranging from 3μm to 50μm. Sodium phosphate in aqueous solution dissociates into positive and negative ions: $Na^+$ and $PO_4^{3-}$. The positive ions will seek out the TMV coat protein's negative charge, surrounding and shielding it and allowing the colloid to be aggregated at higher concentration. Velev and coworkers reported that when the salt concentration increased beyond the critical pinning concentration (CPC), the colloidal particles would adhere to the glass surfaces in sufficient amounts that caused "the contact line pinning" of the solvents[21]. The article reported that the pinning of the contact line was responsible for the formation of shell patterns such as those found in coffee rings. As shown by figure 3.1c, with the absence of electrolyte, stripe formation was not observed and TMV was assembled in random orientation.

Secondly, figure 3.1 shows that the concentration of electrolyte was responsible for the density and percent coverage of the TMV stripes. At low salt concentration, the TMV stripes were present, but less defined. The viruses were assembled and aligned with high percent coverage but in a monolayer fashion. As electrolyte concentration increased, contact line pinning enhanced, leading to increased convection flow toward the liquid surfaces to compensate for the loss of solvents through evaporation. Because solvents evaporate and TMV do not, higher salt concentration, consequently, led to higher TMV concentration at the contact line. The TMV stripes were more well-defined, as evident by the multilayered TMV in figure 3.1b.

Additionally, when the TMV arrays were thoroughly cleaned and washed multiple times with deionized water, AFM showed that the density and orientation of TMV on the glass surfaces still remained the same as before rinsing. Although it has been reported before that the

TMV is attached to the glass surfaces simply by adsorption[8], it is possible that permanent or covalent binding may occur. During plasma cleaning, radicals that were created would react with organic compounds and be removed from the surface by gas flow. In particular, oxygen radicals may form and remain active on the glass surfaces even after the cleaning process. The radicals may react with the TMV coat protein during surface assembly and result in permanent or covalent binding with the TMV. It would be interesting to study the interactions between the TMV coat protein and the glass surfaces, but such examination is beyond the scope of my thesis.

To sum up, results in figure 3.1 illustrate a facile route to control TMV array coverage and alignment by using different concentrations of the TMV and salt for surface assembly.

### 3.2 Effect of temperature on TMV assembly

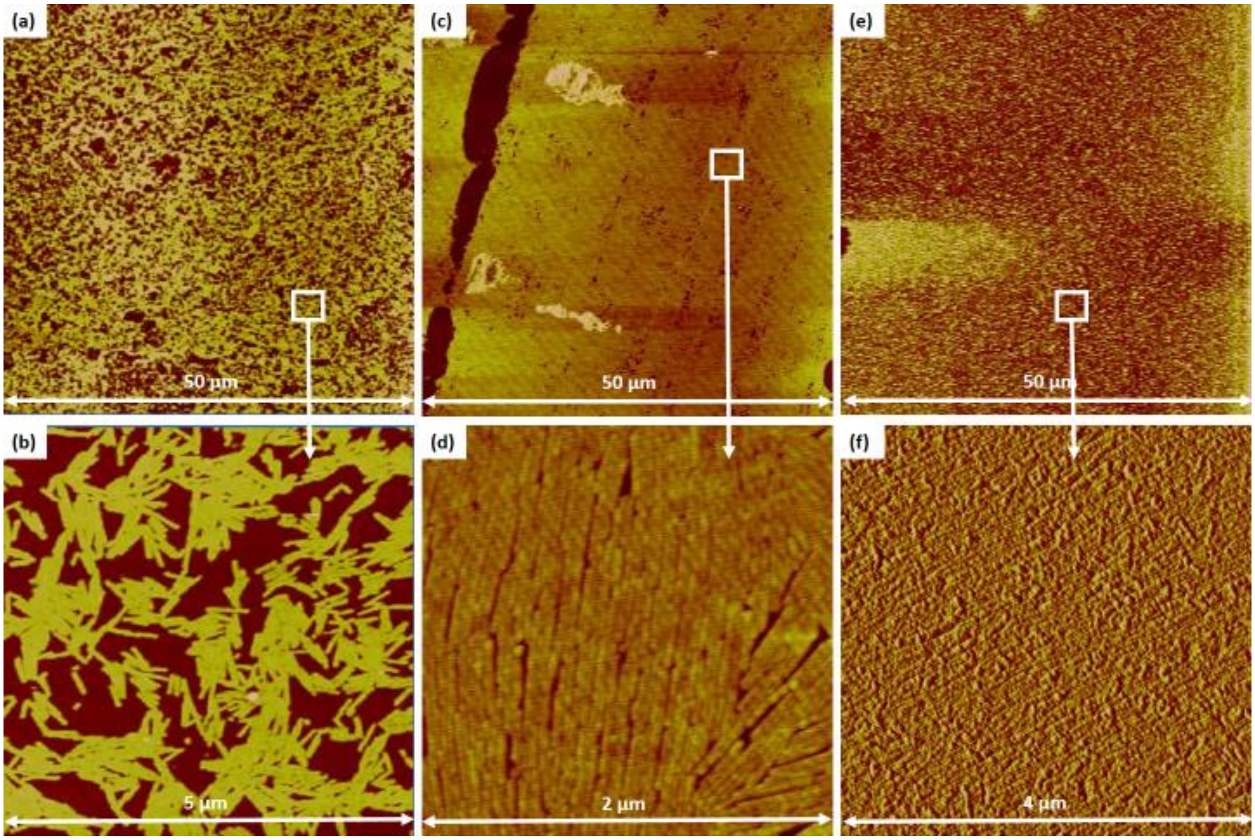


**Figure 3.5:** AFM images (height) of TMV patterns formed on glass slides after the drying of TMV solutions (0.05 mg/mL in 0.01M sodium phosphate) at different temperatures: (a) and (b) 3ºC; (c) and (d) 20ºC; (e) and (f) 50 ºC.

As shown in figure 3.5, I next examined a simple method to control TMV array density, alignment, and percent coverage on glass surfaces by varying the temperature of the system during surface assembly. For all the experiments, TMV solution (0.05 mg/mL in 0.01M sodium phosphate) was injected in between two modified glass slides, and allowed to dry at specific temperatures: 3ºC, 20ºC, or 50ºC. The humidity was controlled to achieve consistent evaporation time of 2.0-2.5 days. As shown in figure 3.5a, when the TMV solution was allowed to dry at 3ºC, the TMV density was very low. At higher magnification (figure 3.5b), the viruses exhibited isotropic distribution and was randomly assembled onto substrate. When the temperature was increased to 20ºC, the TMV density and percent coverage increased significantly (figure 3.5c). Higher magnification AFM image (figure 3.5d) shows that the viruses were also very well aligned and tightly packed throughout the entire TMV stripes. As shown in figure 3.5e, at higher temperature (50ºC), the viruses were assembled with even higher density and coverage. Higher magnification AFM image (figure 3.5f) shows that they were in fact very well aligned despite the overlapping of the TMVs due to their high assembly density.

Figure 3.5 implies that by simply adjusting the temperature of system during TMV assembly, density and coverage of the TMV array can be easily controlled. From a thermodynamic perspective, the assembly of colloidal nanoparticles at the liquid surface is due to the minimization of Gibbs free energy (G) expressed through enthalpy (H), entropy (S), and temperature (T).

$$\Delta G = \Delta H - T\Delta S \qquad (2)$$

Enthalpy is determined by specific interactions between colloidal nanoparticles. These include interactions between TMV protein coats, Columbic, dipole-dipole, and van der Waals[22]. Due to the negative charge of the RNA and the coat proteins, the TMV exhibits low pI of 3.5[11]. At pH of 7.0, the TMV is overall negatively charged. The total interactive energy, created from van der Waals and electrostatic interaction of the TMV, increases significantly as the distance between the viruses decreases[23,24]. Therefore, kinetic energy is required to overcome the repulsive energy and ΔH is positive as the viruses assembled in closer proximity during alignment[25].

When the viruses are at high density, the alignment of TMV involves positive ΔG. This alignment process utilizes the Coffee ring effect which is produced due to the pinning of the contact line onto the substrate by the solute. As explained earlier in section 3.1, the Coffee ring effect causes higher concentration of TMV at the three phase contact line. With higher concentration, Onsager reported that the viruses would appear in nematic distribution for purely "entropic reasons."[27] At high concentration of colloidal rods (such as TMV), free energy is found to be unstable if they are in isotropic distribution with one another[3]. Rotational entropy is maximized when the rods point in all direction with equal probability while translational entropy, or packing entropy, is maximized when the viruses have the maximum free volume. Rotational entropy is indirectly proportional to particle density, while translational entropy is a function of the angle between the TMV (outlined in Onsager model). At lower concentration, rotational entropy dominates and the TMV are suspended in isotropic distribution. At higher TMV concentration, the rotational freedom is restricted by the translational constrains such that "the freedom to rotate restricts the freedom to translate and vice versa." Thus, entropy is maximized when the TMV are aligned in nematic distribution. There were several other reports confirming the Onsager model[15,28-31]. In particular, Grzybowski and coworkers were able to show that nematic distribution occurs at the critical concentration when density of colloidal particles increases beyond $1/(\pi h^2 D)$, where h is the height of the TMV, and D is its diameter[15]. Utilizing the dimension of TMV ($18\times300 nm^2$) and the molecular weight of TMV of approximately 40MDa, the critical concentration of TMV was calculated to be 13 mg/mL (calculations shown in appendix 5.1). Although this value may be an approximation, it shows that the Coffee Ring Effect had to increase the concentration of the TMV at the three phase contact line from 0.05 mg/mL to 13 mg/mL, a 260 fold increase in concentration, in order to achieve nematic distribution and alignment of the TMV.

Because alignment of TMV involves positive enthalpy and positive entropy at high TMV density, equation (2) implies that entropy plays a larger role in the Gibbs free energy at higher temperature. At higher temperature, the repulsive charges of the TMV have less effect on Gibbs free energy, and the TMV can be assembled in closer proximity. This consequently led to higher TMV density and alignment on glass surfaces as shown by figure 3.5e and 3.5f. In summary, the results from figure 3.5 provide the first direct method to regulate TMV array density and alignment by simply controlling the temperature of the system during TMV surface assembly.

### 3.3 Effect of evaporation rate on TMV assembly

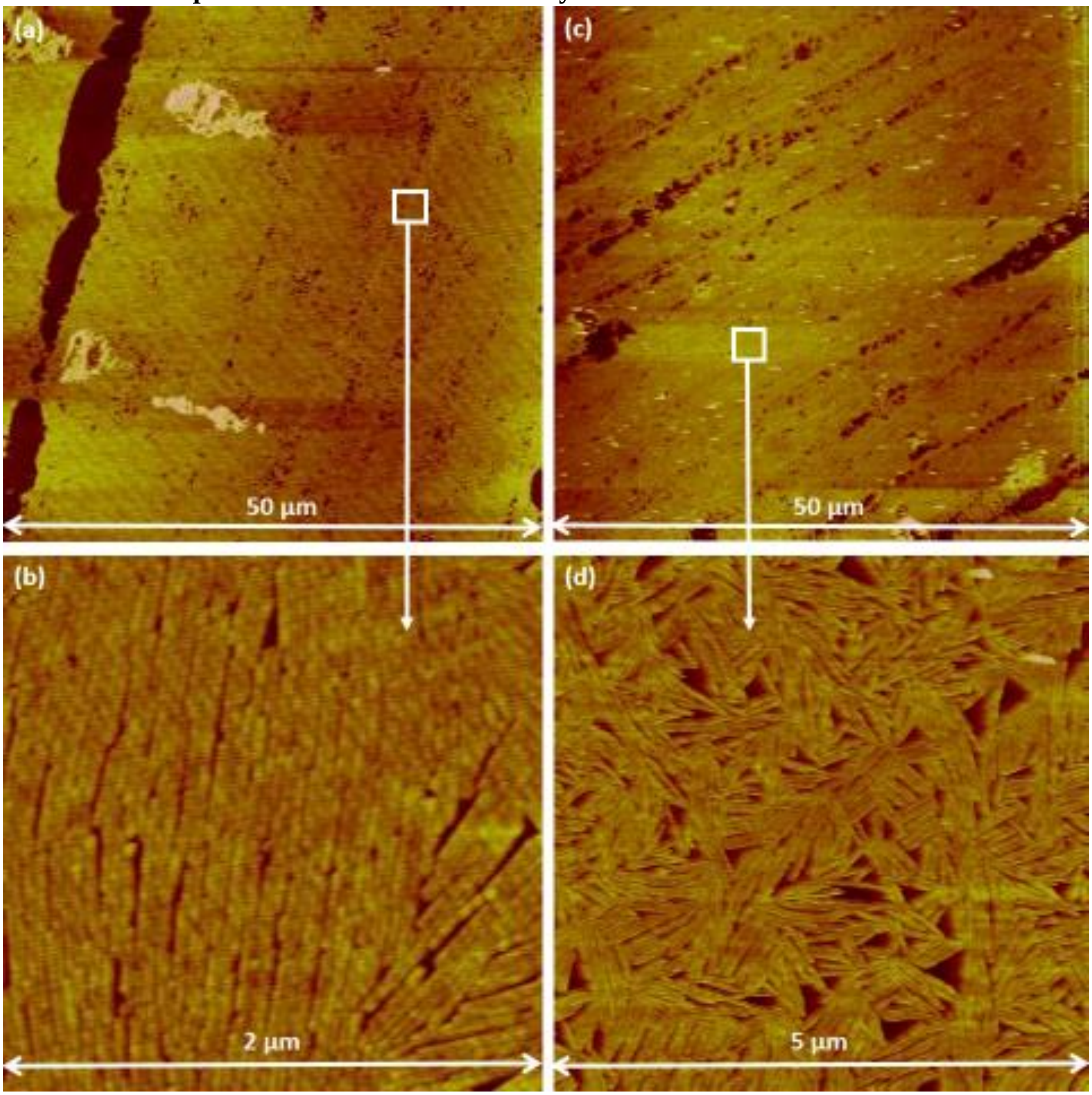


**Figure 3.6:** AFM images (height) of TMV patterns formed on glass slides after the drying of TMV solutions (0.05 mg/mL in 0.01M sodium phosphate) at room temperature with different evaporation times: (a) and (b) 60 hours; (c) and (d) 3 hours.

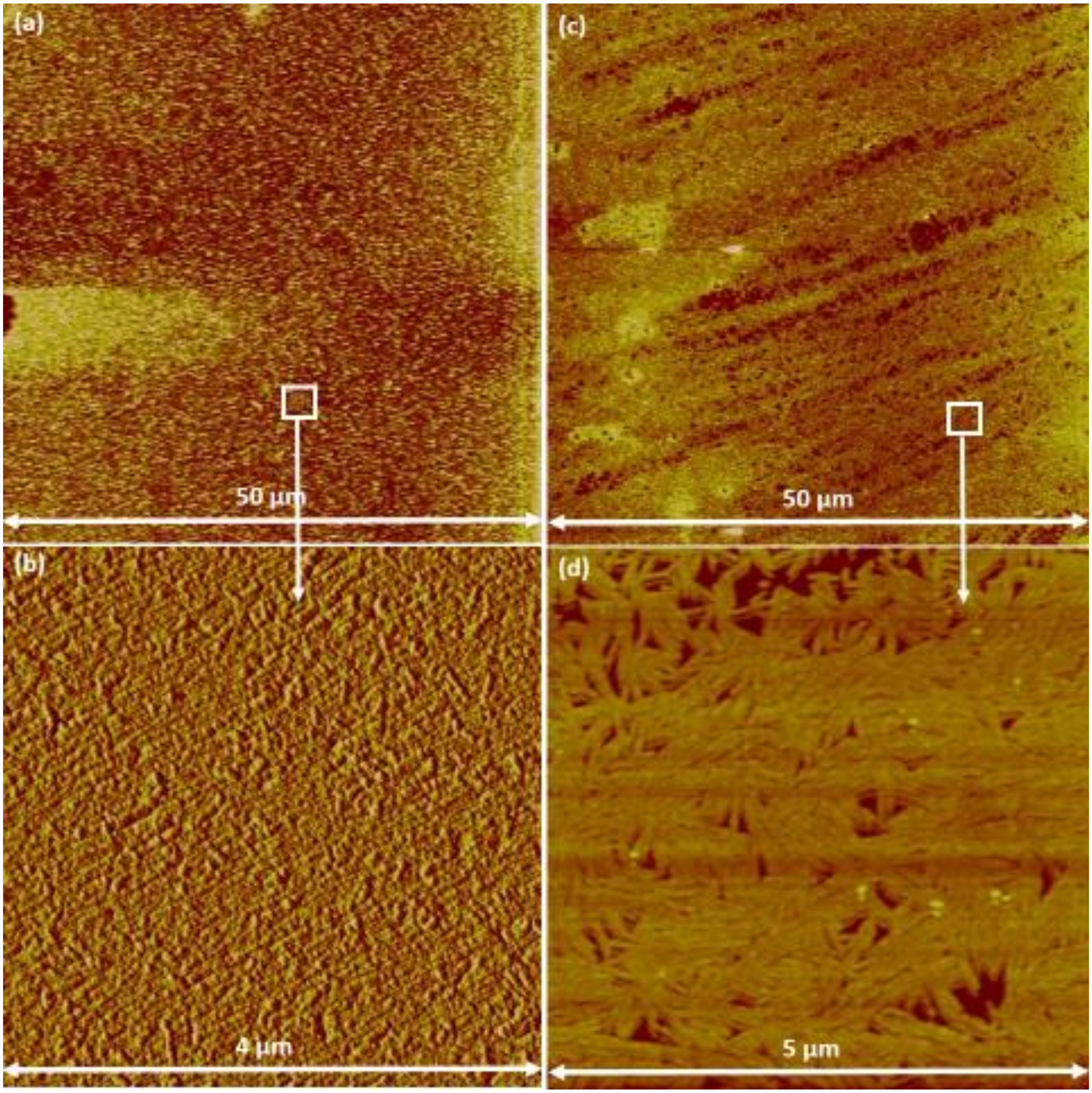


**Figure 3.7:** AFM images (height) of TMV patterns formed on glass slides after the drying of TMV solutions (0.05 mg/mL in 0.01M sodium phosphate) at 50ºC with different evaporation times: (a) and (b) 48 hours; (c) and (d) 3 hours.

As shown in figure 3.6 and 3.7, I also examined a method to control TMV alignment by regulating the rate of evaporation during surface assembly. To control evaporation rate, air humidity was adjusted at different temperatures based on the empirical equation published by Willis Carrier and coworkers (equation 1). At room temperature, when the evaporation time was regulated to be approximately 60 hours, figure 3.4a and 3.4b show that the viruses were assembled with high density and alignment. When evaporation time was lowered to 3 hours, figure 3.4c shows that density of the TMV was only slightly reduced. However, AFM images at higher magnification (figure 3.6d) show that the viruses were in fact randomly assembled. Figure 3.7 demonstrates the effect of evaporation rate on the assembly of TMV at higher temperature - 50ºC. As shown in figure 3.7b and 3.7d, increasing the rate of assembly also resulted in viruses with isotropic distribution.

One possible reason for this behavior can be contributed to the insufficient time allowed for the minimization of the Gibbs free energy. Because the evaporation rates were very high, it was possible that the TMVs were deposited onto the glass surfaces even before they can be arranged in nematic distribution that would maximize entropy. In sum, figure 3.6 and 3.7 suggest that slow evaporation rates were required in order to achieve well-ordered TMV array.

# 4. Conclusion

In my senior honors thesis, I examined two approaches to control the self-assembly of TMV onto glass surfaces. In the first approach, the TMV array density, alignment, and stripe patterns were controlled by regulating the concentrations of TMV and sodium phosphate for the evaporation of TMV solution. Presence of sodium phosphate was necessary for the formation of TMV stripes, while the stripe patterns could be controlled by varying its concentration. In the second approach, the temperature of the system was varied during TMV assembly, leading to direct control over TMV array alignment, density, and percent coverage. When the TMV solution was evaporated at a higher temperature, AFM images showed patterned TMV array with high density and nearly 100% surface coverage. I envision that this method to control the self-assembly of TMV will have great potential in the development of functional devices based on novel nanobio-materials. Indeed, I have conducted further experiments utilizing the work presented here. For instance, I have also been working on developing the formation of TMV-templated palladium nanoclusters on the TMV array, with results that show tunable palladium nanoparticle size and distribution. Carrying this work further will ultimately open new opportunities in developing novel technologies.

# 5. Appendix

## 5.1 Critical TMV Concentration ($C_{TMV}$)

Molecular weight of TMV[1] ~ 40M Da

$C_{TMV}$[5] $= \frac{1}{\pi h^2 D}$ where h is the height and D is the diameter of TMV

$$= \frac{1}{\pi \times 300^2 \times 18} \text{nm}^{-3}$$

$$= \frac{1.96\times10^{-7}}{6.022\times10^{23}} nm^{-3} \times mol\ TMV\ \times 1 \frac{nm^3}{1.0\times10^{-21}\times mL}$$

$$=3.25 \times 10^{-10} \frac{mol\ TMV}{mL} \times \frac{40000000g}{mol\ TMV} \times \frac{1000mg}{1g}$$

$$=13 \frac{mg}{mL}$$

## 5.2 Rate of Evaporation

**Evaporation Flux**

An empirical formula published by Willis Carrier and coworker was used to calculate the rate of evaporation (assuming the concentration of solute is negligible).

$$E = \frac{(0.0888 + 0.0783V)(Pw - Pa)}{hw}$$

Where

E = Evaporation flux [$kg/m^2sec$]; Pw = saturated water vapor partial pressure [Pa]

Pa = water vapor partial pressure of air; hw = the latent heat of vaporization [J/kg]

At room temperature:

| | |
|---|---|
| Pw | = 2300 Pa |
| Pa (50% humidity) | = 1150 Pa |
| V (velocity of air) | = 0 |
| hw (latent heat of evaporation) | =2270000 J/kg |

$$E \quad = \frac{(0.0888 + 0.0783V)(Pw - Pa)}{hw}$$

$$= \frac{((0.0888)(2300-1150)Pa)}{2270000\frac{J}{kg}}$$

$$= 4.50 \times 10^{-5} \times \frac{kg}{m^2 \times sec}$$

$$= 162.0\,\frac{g}{m^2 hr}$$

**Rate of evaporation**

Initial rate of evaporation:

SA = 0.000110m$^2$

Evaporation rate = 0.018g/hr

Maximum evaporation rate:

SA= 0.000134m$^2$

Evaporation rate = 0.022g/hr

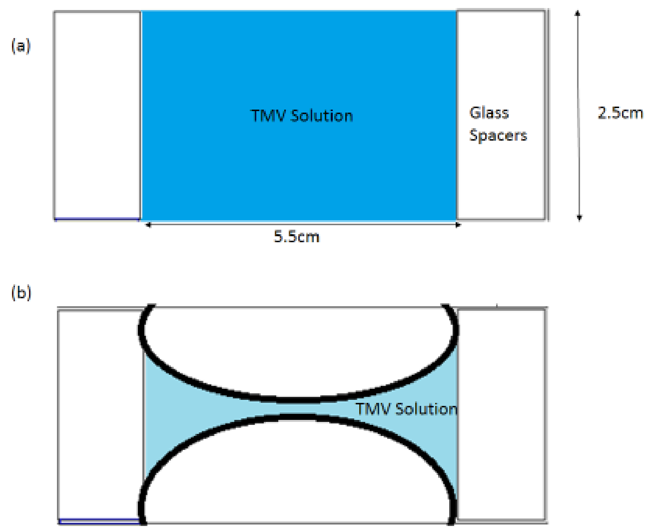


**Figure A.1**: Schematic diagram of TMV solution (represented by blue) confined in between two glass slides at (a) time=0 and (b) time at maximized evaporation rate

Therefore, at room temperature and 50% humidity, the process would require approximately 2.9 days in order to completely evaporate 1.4mL of water.

## 6. References


1. Kuncicky, D.M.; Naik, R.R.; Velev, O.D. *Small*, **2006**. 2(12): p.1462-1463.
2. Yang, C.; Yi, H. *Biochemical Engineering Journal*, **2010**. 52: p. 160-167.
3. Bruckman, M.A.; Liu, J.; Koley, G.; Li, Y.; Benicewicz, B.; Niu, Z.; Wang, Q. *Journal of Materials Chemistry*, **2010**. 20: p. 5715-5719.
4. Rego, J.M.; Yi, H. *Supramolecular Chemistry: From Molecules to Nanomaterials*, **2012**: p. 2275-2291.
5. Britt, D. W.; Buijs, J.; Hlady, V. *Thin Solid Films* **1998**. 824: p. 327-329.
6. Knez, M.; Sumser, M. P.; Bittner, A. M.; Wege, C.; Jeske, H.; Hoffmann, D. M. P.; Kuhnke, K.; Kern, K. *Langmuir* **2003**, 20: p. 441.
7. He, J.; Niu, Z.; Tangirala, R.; Wang, J.-Y.; Wei, X.; Kaur, G.; Wang, Q.; Jutz, G.; Bker, A.; Lee, B.; Pingali, S. V.; Thiyagarajan, P.; Emrick, T.; Russell, T. P. *Langmuir,* **2009**. 25: p. 4979.
8. Lin, Y.; Su, Z.; Xiao, G.; Balizan, E.; Kaur, G.; Niu, Z.; Wang, Q. *Langmuir* **2011**, 27: p. 1398.
9. Lin, Y.; Balizan, E.; Lee, L. A.; Niu, Z.; Wang, Q. *Angewandte Chemie International Edition* **2010**, 49: p. 868.
10. Peng, B.; Liu N.; Lin, Y.; Wang, L.M.; Zhang, W.K.; Niu, Z.W.; Wang, Q.; Su, Z.H., *Sci China Chem*, **2011**. 54(1): p. 137-143
11. Khan, A.A.; Fox, E.K.; Gorzny, M.L.; Nikulina E.; Brougham D.F.; Wege C.; Bittner A.M., *Langmuir*, **2013**. 29: p. 2094-2098
12. Lee, S.Y.; Royston, E.; Culver J.N.; Harris M.T.; *Nanotechnology*, **2005**. 16: p. S435-S441
13. H. Fraenkelconrat; R. C. Williams, *Proc. Nat. Acad. Sci.* 1955. **41**: p.690

14. Deegan, R.D.; Bakajin, O.; Dupont, T.F.; Huber, G.; Nagel, S.R.; Witten, T.A., *Nature* **1997**. 389, p. 827-829.
15. Bishop, K.J.M.; Wilmer C.E.; Soh S.; Grzybowski, B.A., *Small*, **2009**. 5 (14): p. 1600-1630
16. Nunez, M.E., *Nunez Group Research.*
17. Carrier,W.H., *Transactions of Am. Soc. Of Heat. & Vent. Engineers*, **1923.** 24: p. 25-50.
18. Li, Z.; Heiselberg, P., Aalborg University Department of Building Technology and Structural Engineering. **2005**
19. Sartori, E. *Solar Energy*, **1999**. 68 (1): p.77-89.
20. Knez, M; Sumser, M.P.; Bittner, A.M.; Wege, C.; Jeske H.; Hoffman, D.M.P; Kuhnke, K.; Kern, K., *Langmuir*, **2004**. 20: p. 441-447.
21. Kuncicky, D.M.; Velev, O.D., *Langmuir* **2008**, 24: p.1371-1380.
22. Bodnarchuk, M. I.; Kovalenko, M. V.; Heiss, W.; Talapin D.V., *J. American Chemical Society*, **2010**. 132: p.11967-11977
23. Lee, S.Y.; Culver, J.N.; Harris M.T., *Journal of Colloid and Interface Science*, **2006.** 297(2): p. 554-560.
24. Lee, S.Y.; Lim, J.S.; Culver, J.N.; Harris, M.T., *Journal of Colloid and Interface Science*, **2008**. 324(1-2): p.92-98.
25. Levine, I.N., “Physical Chemistry.” *Mcgraw Hill*, **2009**. 6: p. 672-729
26. Sharma, O.P., “Textbook of Fungi.” *Mcgraw Hill*, **1989**. 1: p. 327
27. Onsager, L. *Annals of the New York Academy of Science*, **1949**. 51: p. 627-659.
28. Straley, J.P. *Mol Cryst Liq Cryst*, **1973**. 22: p. 333 – 57.

29. Forsyth, P.A.; Marcelja, S., Mitchell, D.J.; Ninham, B.W.; *Adv Colloid Interface Sci*, **1978**. 9: p. 37 – 60.

30. Gelbart, W.M. *J Phys Chem*, **1982**. 86: p. 4298 – 307.

31. Dogic, Z.; Fraden, S. *Colloid and Interface Science*, **2006**: p. 47-55.